# Chapter 12
# On the Fractal Dimension of Rough Surfaces

**Bo Persson**

**Abstract** Most natural surfaces and surfaces of engineering interest, e.g., polished or sand blasted surfaces, are self affine fractal over a wide range of length scales, with the fractal dimension $D_f = 2.15 \pm 0.15$. We give several examples which illustrate this and a simple argument, based on surface fragility, for why the fractal dimension usually is $<2.3$. A kinetic model of sand blasting is presented, which gives surface topographies and surface roughness power spectra in good agreement with experiments.

## 12.1 Introduction

All natural surfaces and surfaces of engineering interest have surface roughness on many different length scales, sometimes extending from atomic dimensions to the linear size of the object under study. Surface roughness is of crucial importance in many engineering applications, e.g., in tribology [1–4]. For example, the surface roughness on a road surface influences the tire-road friction or grip [1]. It is therefore of great interest to understand the nature of roughness of surfaces of engineering interest. Several studies of the fractal properties of surface roughness have been presented, but mainly for surfaces produced by growth (atomic deposition) processes [5]. Many studies of surfaces produced by atomistic erosion processes, e.g., sputtering, have also been presented, see, e.g., [6–8]. In this article I will present several examples of power spectra of different surfaces with self-affine fractal-like surface roughness. All surfaces have fractal dimensions $D_f = 2.15 \pm 0.15$ and I will give a simple argument, based on surface fragility, for why the fractal dimension usually is $<2.3$. I also present a kinetic model of sand blasting which gives surface topographies and surface roughness power spectra in good agreement with experiments.

B. Persson (✉)
Peter Grünberg Institut, Forschungszentrum Jülich, 52425 Jülich, Germany
e-mail: b.persson@fz-juelich.de

## 12.2 Power Spectrum: Definition

We consider randomly rough surfaces where the statistical properties are transitionally invariant and isotropic. In this case the 2D power spectrum [3, 9]

$$C(\mathbf{q}) = \frac{1}{(2\pi)^2} \int d^2x \ \langle h(\mathbf{x})h(\mathbf{0})\rangle e^{-i\mathbf{q}\cdot\mathbf{x}}$$

will only depend on the magnitude $q$ of the wavevector $\mathbf{q}$. Here $h(\mathbf{x})$ is the height coordinate at the point $\mathbf{x} = (x, y)$ and $\langle .. \rangle$ stands for ensemble averaging. From $C(q)$ many quantities of interest can be directly calculated. For example, the root-mean-square (rms) roughness amplitude $h_{\mathrm{rms}}$ can be written as

$$h_{\mathrm{rms}}^2 = 2\pi \int_{q_0}^{q_1} dq \ q C(q) \tag{12.1}$$

where $q_0$ and $q_1$ are the small and large wavevector cut-off. The rms-slope $\kappa$ is determined by

$$\kappa^2 = 2\pi \int_{q_0}^{q_1} dq \ q^3 C(q). \tag{12.2}$$

For a self affine fractal surface

$$C(q) = C_0 \left(\frac{q}{q_0}\right)^{-2(1+H)} \tag{12.3}$$

Substituting this in (12.1) gives

$$h_{\mathrm{rms}}^2 = \frac{\pi C_0}{H} q_0^2 \left[1 - \left(\frac{q_1}{q_0}\right)^{-2H}\right] \tag{12.4}$$

and from (12.2) we get

$$\kappa^2 = \frac{\pi C_0}{1 - H} q_0^4 \left[\left(\frac{q_1}{q_0}\right)^{2(1-H)} - 1\right] \tag{12.5}$$

Usually $q_0/q_1 \ll 1$ and since $0 < H < 1$, unless $H$ is very close to 0 or 1, we get

$$\kappa = q_0 h_{\mathrm{rms}} \left(\frac{H}{1 - H}\right)^{1/2} \left(\frac{q_1}{q_0}\right)^{1-H} \tag{12.6}$$

Many surfaces of engineering interest, e.g., a polished steel surface, have rms-roughness of order $\sim 1\,\mu\text{m}$ when probed over a surface region of linear size $L = \pi/q_0 \sim 100\,\mu\text{m}$. This gives $q_0 h_{\text{rms}} \approx 0.1$ and if the surface is self affine fractal the whole way down to the nanometer region (length scale $a$) then $q_1 = \pi/a \approx 10^{10}\,\text{m}^{-1}$ and (12.6) gives $\kappa \approx 0.1 \times 10^{5(1-H)}$. I use this equation to argue that most surfaces of interest, if self affine fractal from the macroscopic length scale (say $L \sim 100\,\mu\text{m}$) to the nanometer region, cannot have a fractal dimension larger than $D_{\text{f}} \approx 2.3$ or so, as otherwise the average surface slope becomes huge which is unlikely to be the case as the surface would be very "fragile" and easily damaged (smoothed) by the mechanical interaction with external objects. That is, if we assume that the rms slope has to be below, say [3], we get that $H > 0.7$ or $D_{\text{f}} = 3 - H < 2.3$. As we now show, this inequality is nearly always satisfied for real surfaces.

## 12.3 Power Spectra: Some Examples

I have calculated the 2D surface roughness power spectra of several hundred surfaces of engineering interest. Here I give just a few examples to illustrate the general picture which has emerged. Figure 12.1 shows the 2D power spectrum of a sand blasted PMMA surface obtained from 1D-stylus height profiles. The surface is self-affine fractal for large wavevectors and the slope of the dashed line corresponds to the Hurst exponent $H = 1$ or fractal dimension $D_{\text{f}} = 2$. For $q < q_{\text{r}} \approx 10^4\,\text{m}^{-1}$ (corresponding to the roll-off wavelength $\lambda_{\text{r}} = \pi/q_{\text{r}} \approx 100\,\mu\text{m}$) the power spectrum exhibits a roll-off which, however, moves to smaller wavevectors as the sand blasting time period increases (not shown).
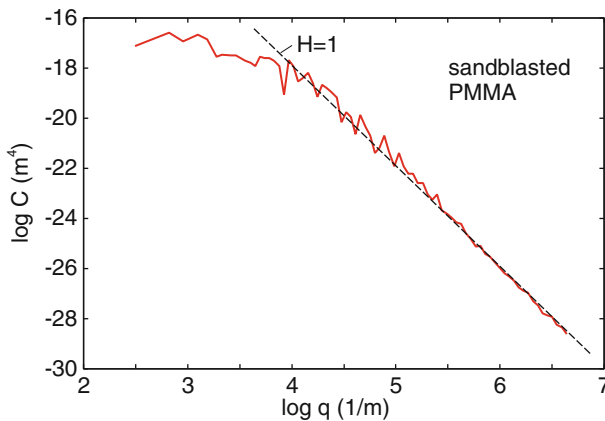


**Fig. 12.1** The 2D power spectrum of a sand blasted PMMA surface based 1D-stylus height profiles [10] ($\log_{10} - \log_{10}$ scale). The slope of the *dashed line* corresponds to the Hurst exponent $H = 1$ or fractal dimension $D_{\text{f}} = 2$
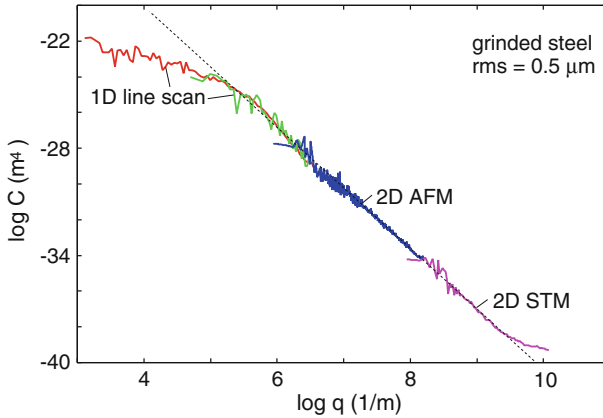
**Fig. 12.2** The 2D power spectra of grinded steel surface [11]. The slope of the *dashed line* correspond to the Hurst exponent $H = 0.72$ or fractal dimension $D_f = 2.28$

Figure 12.2 shows the angular averaged power spectrum of a grinded steel surface. The surface topography was studied on different length scales using STM, AFM and 1D stylus. Note that the (calculated) power spectra using the different methods join smoothly in the wavevector regions where they overlap. The slope of the dashed line corresponds to the Hurst exponent $H = 0.72$ or fractal dimension $D_f = 2.28$

Figure 12.3 shows the power spectra of two asphalt road surfaces. Both surfaces are self-affine fractal for large wavevectors and exhibit a roll-off for small wavevectors which is related to the largest stone particles (diameter $d$) in the asphalt via $q_r \approx \pi/d$. The fractal dimension of both surfaces are $D_f \approx 2.20$.
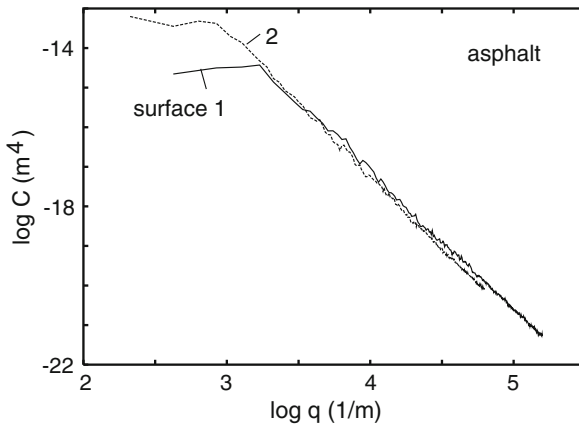


**Fig. 12.3** The 2D power spectra of asphalt road surface [12]. The slope of the *dashed line* correspond to the Hurst exponent $H = 0.80$ or fractal dimension $D_f = 2.20$
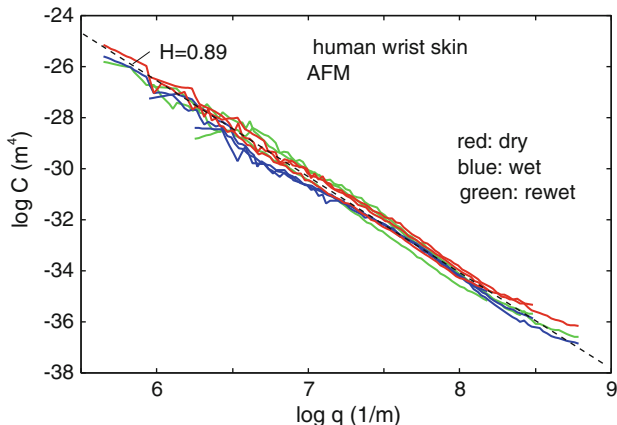
**Fig. 12.4** The 2D power spectrum of human wrist skin obtained from AFM measurements [13]. The rms roughness is $h_{rms} \approx 0.25\,\mu m$ within the studied wavevector region. The slope of the *dashed line* corresponds to the Hurst exponent $H = 0.89$ or fractal dimension $D_f = 2.11$

Not only surfaces prepared by engineering methods (e.g., sand blasting or polishing) exhibit self-affine fractal properties with fractal dimensions $D_f = 2.15 \pm 0.15$ but so do most natural surfaces. Thus, for example, surfaces prepared by crack propagation are usually self affine fractal with $D_f \approx 2.2$. Here I give three more examples to illustrate this. Figure 12.4 shows the 2D power spectrum of human wrist skin obtained from AFM measurements. The rms roughness is $h_{rms} \approx 0.25\,\mu m$ in the studied wavevector region. The slope of the dashed line corresponds to the Hurst exponent $H = 0.89$ or fractal dimension $D_f = 2.11$. Figure 12.5 shows 2D power
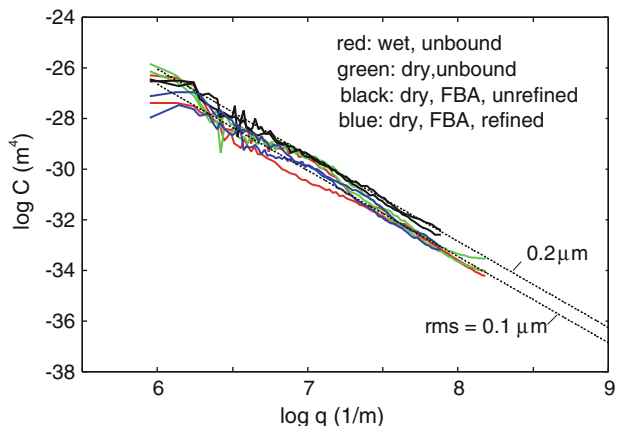


**Fig. 12.5** The 2D power spectra of dry and wet cellulose fibers [15]. The surface topography was measured using AFM. The slope of the *dashed lines* correspond to the Hurst exponent $H = 0.7$ or fractal dimension $D_f = 2.3$
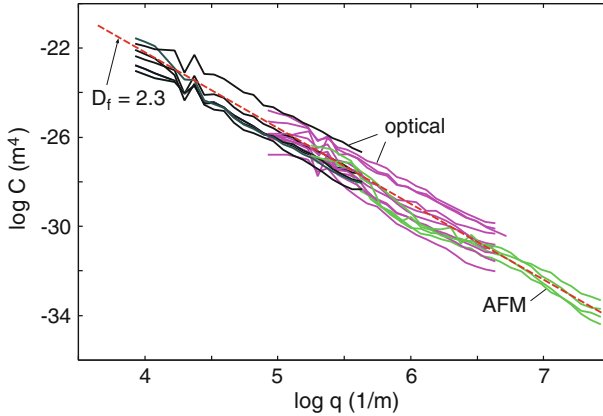
**Fig. 12.6** The 2D power spectrum of pulled adhesive tape based on optical and AFM measurements [16]. The slope of the *dashed line* corresponds to the Hurst exponent $H = 0.7$ or fractal dimension $D_f = 2.3$

spectra of dry and wet cellulose fibers measured using AFM. The slope of the dashed lines correspond to the Hurst exponent $H = 0.7$ or fractal dimension $D_f = 2.3$. Finally, Fig. 12.6 shows the 2D power spectrum of pulled adhesive tape based on optical and AFM measurements. The slope of the dashed line corresponds to the Hurst exponent $H = 0.7$ or fractal dimension $D_f = 2.3$.

I have shown above that many engineering and natural surfaces exhibit self-affine fractal properties in a large wavevector range with fractal dimension $D_f = 2.15 \pm 0.15$. A fractal dimension larger than $D_f = 2.3$ is unlikely as it would typically result in surfaces with very large rms-slope, and such surfaces would be "fragile" and easily smoothed by the (mechanical) interaction with the external environment. However, this argument does not hold if the surface is self-affine fractal in a small enough wavevector region or if the prefactor $C_0$ in the expression $C(q) = C_0 (q/q_0)^{-2(1+H)}$ is very small. In fact, self affine fractal surfaces with the fractal dimension $D_f = 3$ result when a liquid is cooled below its glass transition temperature where the capillary waves on the liquid surface gets frozen-in. For capillary waves (see, e.g., [2]):

$$C(q) = \frac{1}{(2\pi)^2} \frac{k_B T}{\rho g + \gamma q^2} \tag{12.7}$$

where $\rho$ is the mass density, $g$ the gravitation constant and $\gamma$ the liquid surface tension. For $q \gg q_0 = (\rho g/\gamma)^{1/2}$ we have $C(q) \sim q^{-2}$ and comparing this with the expression for a self affine fractal surface $C(q) \sim q^{-2(1+H)}$ gives $H = 0$ and $D_f = 3$. In a typical case the cut-off $q_0 \approx 10^3$ m$^{-1}$ is rather small, but the rms roughness and the rms slope are still rather small due to the smallness of $C_0 = k_B T/\rho g$, which results from the small magnitude of thermal energy $k_B T$. Using AFM, frozen capillary waves have recently been observed on polymer surfaces (polyaryletherketone, with the glass transition temperature $T_g \approx 423$ K and $\gamma \approx 0.03$ J/m) [18], see also [17].

The measured power spectrum was found to be in beautiful agreement with the theory prediction of (12.7). For this case, including all the roughness with $q > q_0$, one can calculate the rms roughness to be $h_{rms} \approx (k_B T/2\pi\gamma)^{1/2}[\ln(q_1/q_0)]^{1/2} \approx 1$ nm and the rms slope $\kappa \approx (k_B T/4\pi\gamma)^{1/2} q_1 \approx 1$.

## 12.4 Simulation of Rough Surfaces: A Simple Erosion Process

I have argued above that if a surface is self affine fractal over a large wavevector region (as it is often the case) it usually has a fractal dimension <2.3, since otherwise the rms-slope would be so large ($\gg 1$) as to make the surface fragile, and very sensitive to the impact of external objects which would tend to smooth the surface. Here I will consider a simple model of sand blasting, showing that if one assumes that material removal is more likely at the top of asperities rather than in the valleys (see Fig. 12.7), a surface with relatively low fractal dimension is naturally obtained. The model studied here has some similarities with growth models involving random deposition with surface relaxation. However, instead of adding atoms or particles I consider removal of material. In addition, while in growth models the surface relaxation is usually interpreted as a diffusive (thermal) motion of atoms, in the present case thermal effects are not directly involved (but may be indirectly involved in determining if the material removal involves plastic flow or brittle fracture).

We now present a model for sand blasting, where a beam of hard particles is sent on the surface orthogonal to the originally flat substrate surface, and with a laterally uniform probability distribution. The substrate is considered as a cubic lattice of
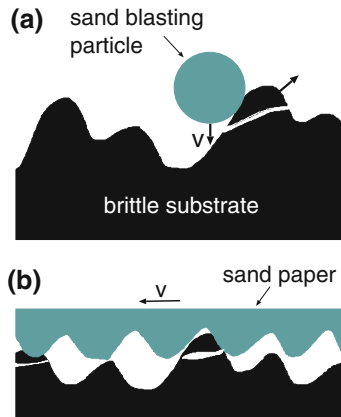


**Fig. 12.7** Sand blasting (**a**) and lapping with sand paper (**b**) will roughen an initially flat surface but in such a way that high and sharp asperities never form i.e., the removal of material is easier at the top of asperities than at the valley. This will result in a rough surface with low fractal dimension
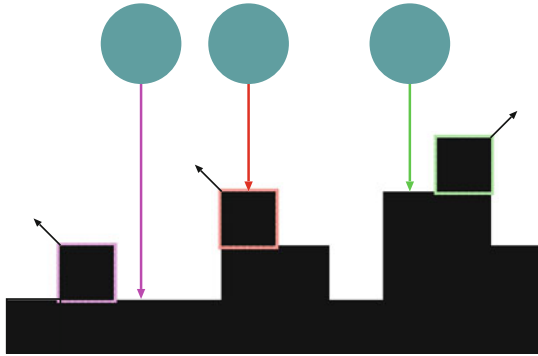
**Fig. 12.8** Incoming particles (*arrows*) and the blocks removed by the impact (*black squares* surrounded by colored rims) for a 1D version of the simulation model used. For the 2D model I use, if a particle impact at site $(i, j)$ (at position $(x, y) = (i, j)a$, where $a$ is the lattice constant) then one of the blocks $(i, j)$, $(i + 1, j)$, $(i - 1, j)$, $(i, j + 1)$ or $(i, j - 1)$ is removed. Of these blocks I assume that either the block which has the smallest number of nearest neighbors is removed (with probability 0.5), since this block is most weakly bound to the substrate, or the highest block is removed (with probability 0.5). In both cases, if several such blocks exist I choose randomly the one to be removed unless the block $(i, j)$ is part of the set of blocks, in which case this block is removed

blocks (or particles) and every particle from the incoming beam removes a randomly chosen surface block on the solid substrate. As shown in Fig. 12.8, if an incoming particle impacts at site $(i, j)$ (at position $(x, y) = (i, j)a$, where $a$ is the lattice constant) then one of the blocks $(i, j)$, $(i + 1, j)$, $(i - 1, j)$, $(i, j + 1)$ or $(i, j - 1)$ is removed. Of these blocks I assume that either (a) the block which has the smallest number of nearest neighbors is removed (with probability 0.5), since this block is most weakly bound to the substrate, or (b) the highest located block is removed (with probability 0.5). In both cases, if several such blocks exist I choose randomly the one to remove unless the block $(i, j)$ is part of the set of blocks, in which case this block is removed. The substrate surface consists of $2048 \times 2048$ blocks and I assume periodic boundary conditions. We note that the processes (a) and (b) above are similar to the Wolf-Villain [19] and Family [20] grows models, respectively.

Figure 12.9 shows the topography of a surface produced by the eroding process described above (see also Fig. 12.8), after removing 76290 layers of blocks. The surface topography is practically undistinguished from that of sand blasted surfaces (not shown). Figure 12.10 shows the surface roughness power spectrum as a function of the wavevector (on a $\log_{10} - \log_{10}$ scale). The surface is self affine fractal with the Hurst exponent $H = 1$ (or fractal dimension $D_f = 2$), which has also been observed for sand blasted surfaces (see Fig. 12.1). Even the magnitude of $C(q)$ predicted by the theory is nearly the same as observed (see Fig. 12.1). For more results from simulations of surfaces roughened by erosion, see the Appendix.
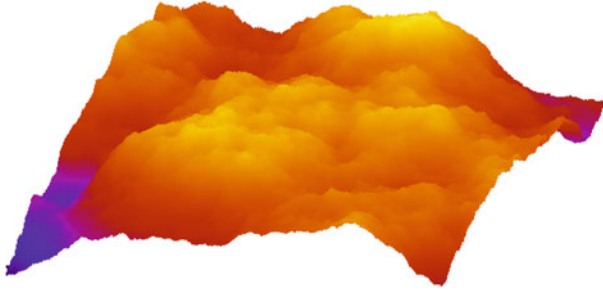
**Fig. 12.9** Topography picture of a surface produced by the eroding process described in Fig. 12.8 after removing 76,290 layers of blocks. The surface plane consists of $2,048 \times 2,048$ blocks. The surface is self affine fractal with the Hurst exponent $H = 1$ (or fractal dimension $D_f = 2$) (see Fig. 12.10). The width of the removed particles (or blocks) is $a = 0.1\ \mu$m. The surface has the rms roughness $h_{rms} = 2.1\ \mu$m and the rms slope $\kappa = 1.04$
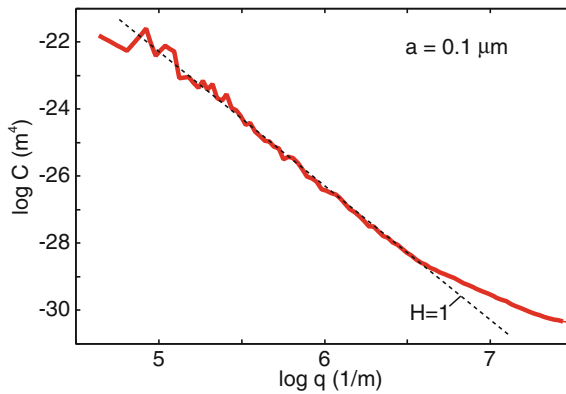


**Fig. 12.10** The surface roughness power spectrum as a function of the wavevector ($\log_{10} - \log_{10}$ scale) after removing 76,290 layers of blocks (surface topography in Fig. 12.9). The surface plane consists of $2,048 \times 2,048$ blocks. The surface is self-affine fractal with the Hurst exponent $H = 1$ (or fractal dimension $D_f = 2$). We have assumed the linear size of the removed blocks to be $a = 0.1\ \mu$m

## 12.5 Discussion and Summary

Surface roughness on engineering surfaces is important for a large number of properties such as the heat and electric contact resistance [21, 22], for mixed lubrication [23], wear and adhesion [24]. Thus, for example, one standard way to reduce adhesion is to roughen surfaces. In wafer bonding one instead wants the surfaces to be as smooth as possible and already surface roughness of order a few nanometer (when measured over a length scale of $\sim 100\ \mu$m) may eliminate adhesion.

Surfaces produced by brittle crack propagation tend to be self-affine fractal with the fractal dimension $D_f \approx 2.2$, but no generally accepted theory exists which can
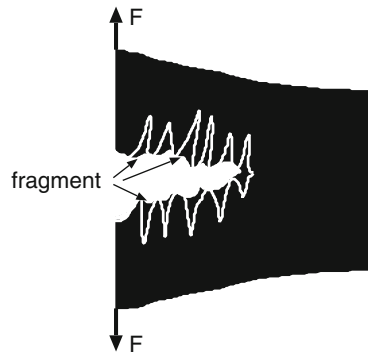
**Fig. 12.11** Brittle fracture usually produces self-affine fractal surfaces with the fractal dimension $D_f \approx 2.2$. If (hypothetically) the fractal dimension would be much higher the surface slope would be very high too, which would result in sharp asperities broken-off forming fragments localized at the fracture interface

explain why [25, 26]. Fractured surfaces are usually very rough on macroscopic length scales. If such surfaces would have the fractal dimension $D_f > 2.3$ they would have huge rms-slope, i.e., very sharp asperities would appear at short enough length scales. It is intuitively clear that sharp asperities cannot form as they would not survive the cracking process, but would result in fragments of cracked material at the interface (see Fig. 12.11).

The argument presented in this paper for why the fractal dimension is close to 2 for most engineering surfaces assumes that the surfaces are produced by the mechanical interaction between solids and that the surfaces are fractal-like in a wide range of length scales. Many examples of surfaces with fractal dimension $D_f \approx 2.5$ or larger exist. For example, the surfaces resulting from electroreduction of Pd oxide layers have the fractal dimension $D_f \approx 2.57$ (see [27]). In this case no mechanical interaction with external objects (which could smooth the surface) has occurred. In addition, because of the relative thin oxide layer of the untreated surface, the self-affine fractal properties will only extend over a relative small range of length scales. Similarly, electrodeposition may result in surfaces with fractal dimension much larger than 2. Erosion by ion bombardment or exposure of a surface to plasma is another way of producing rough surfaces with self-affine fractal properties. In [8] it was shown that exposing a gold surface to oxygen or argon plasma produced self affine fractal surfaces with the fractal dimension $D_f = 2.1 \pm 0.1$. Ion bombardment (sputtering) of an iron surface produced a surface which was self-affine fractal over two decades in length scales (from 3 to 300 nm) with the fractal dimension $D_f = 2.47 \pm 0.02$ (see [7]). It is not obvious why the the gold and iron surfaces exhibit different fractal properties, but it may be related to the much higher mobility of Au atoms on gold as compared to Fe atoms on iron, which would tend to smooth the gold surface more than the iron surface [28].

To summarize, I have shown that most natural surfaces and surfaces of engineering interest, e.g., polished or sand blasted surfaces, are self affine fractal in a wide range

of length scales, with typical fractal dimension $D_f = 2.15 \pm 0.15$. I have argued that the fractal dimension of most surfaces <2.3, since surfaces with larger fractal dimension have huge rms-slopes and would be very fragile and easily smoothed by the interaction with external objects. I have also presented a simple model of sand blasting and showed that the erosion process I used results in self-affine fractal surfaces with the fractal dimension $D_f = 2$, in good agreement with experiments.

It is clear that a good understanding of the nature of the surface roughness of surfaces of engineering and biological interest, is of crucial importance for a large number of important applications.

# Appendix

Here I present some more results related to simulation of rough surfaces by erosion processes. Consider first the most simple picture of sand blasting where a beam of hard particles is sent on the surface orthogonal to the originally flat substrate surface, and with a laterally uniform probability distribution. The substrate is considered as a cubic lattice of blocks (or particles) and every particle from the incoming beam removes a randomly chosen surface block on the solid substrate. This process, which is similar to the random deposition model [5], will result in an extremely rough substrate surface with the Hurst exponent $H = -1$ and fractal dimension $D_f = 4$. This follows at once from the fact that the power spectrum of the generated surface is independent of the wavevector i.e., $C(q) = C_0$ (a constant) and using the definition $C(q) \sim q^{-2(1+H)}$ we get $H = -1$. The fact that $C(q)$ is constant in this case follows from the fact that the height $h(\mathbf{x})$ is uncorrelated with $h(\mathbf{0})$ for $\mathbf{x} \neq \mathbf{0}$. That is, $\langle h(\mathbf{x})h(\mathbf{0}) \rangle = \langle h(\mathbf{x}) \rangle \langle h(\mathbf{0}) \rangle = 0$ for $\mathbf{x} \neq \mathbf{0}$. Thus we get

$$C(q) = \frac{1}{(2\pi)^2} \int d^2x \, \langle h(\mathbf{x})h(\mathbf{0}) \rangle e^{-i\mathbf{q} \cdot \mathbf{x}} \sim \langle h^2(\mathbf{0}) \rangle$$

Let us now consider the erosion processes (a), (b) and (a + b) discussed in Sect. 12.4. In Fig. 12.12 we show the power spectrum after removing 76,290, 19,070 and 2,384 layers of blocks assuming process (a + b). For short time of sand blasting a large roll-off region prevails which decreases towards zero as the sand blasting time increases. The same effect is observed in experiments (not shown) and reflects the fact that the correlation length $\xi$ along the surface caused by the sand blasting extends only slowly as the sand blasting time $t$ increases (as a power law $\xi \sim t^{1/z}$, see [5]).

In Fig. 12.13 I compare the surface roughness power spectrum as obtained using the random removal model with the random removal with relaxation models (a), (b) and ((a+b) (see Sect. 12.4) after removing 19,070 layers of blocks. The corresponding topography pictures for processes (a), (b) and ((a + b) are shown in Fig. 12.14. Note
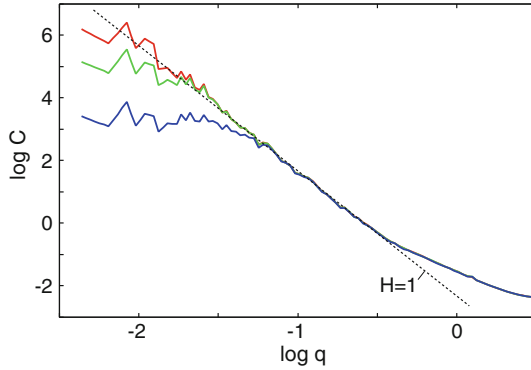
**Fig. 12.12** The surface roughness power spectrum as a function of the wavevector ($\log_{10} - \log_{10}$ scale) for the erosion process (a + b), after removing 2,384 (*blue*), 19,070 (*green*) and 76,290 (*red*) layers of blocks. The wavevector is in units of $1/a$ and the power spectrum is in units of $a^4$
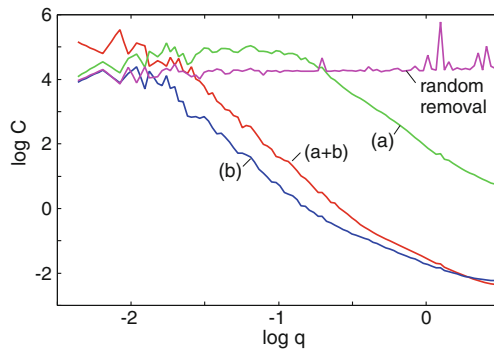
**Fig. 12.13** The surface roughness power spectrum as a function of the wavevector ($\log_{10} - \log_{10}$ scale) for all the erosion processes considered, after removing 19,070 layers of blocks. The wavevector is in units of $1/a$ and the power spectrum is in units of $a^4$

that the random removal process gives a constant power spectrum which I have never observed for any real surface. The random removal with relaxation model (a) gives also unphysical surface topography with high sharp spikes. The ((a + b)) model gives results in agreement with experiments, which shows, as expected, that both removal of high regions (asperity tops) and low coordinated surface volumes are important in sand blasting.

Note that random removal results in an interface which is uncorrelated (see above). The columns shrink independently, as there is no mechanism that can generate correlations along the interface. The other erosion processes [(a), (b) and ((a + b)] all involve correlated removal of material, allowing the spread of correlation along the surface.
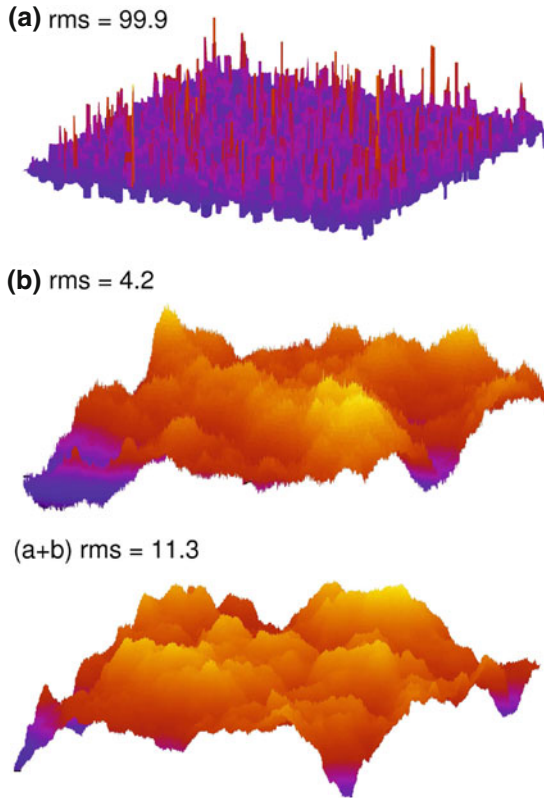
**Fig. 12.14** Topography picture of surfaces produced by the eroding processes (a), (b) and (a + b) after removing 19,070 layers of blocks. The surface plane consist of $2{,}048 \times 2{,}048$ blocks. The rms roughness values are in units of $a$. Random removal without relaxation gives an extremely rough surface (not shown) with the rms roughness $h_{\mathrm{rms}} = 1{,}264a$

## References

1. B.N.J. Persson, J. Chem. Phys. **115**, 3840 (2001)
2. B.N.J. Persson, Surf. Sci. Rep. **61**, 201 (2006)
3. B.N.J. Persson, O. Albohr, U. Tartaglino, A.I. Volokitin, E. Tosatti, J. Phys. Condens. Matter **17**, R1 (2005)
4. J. Krim, Adv. Phys. **61**, 155 (2012)
5. A.L. Barabasi, H.E. Stanley, *Fractal Concept in Surface Growth* (Cambridge University Press, Cambridge, 1995)
6. J. Krim, G. Palasantzas, Int. J. Modern Phys. B **9**, 599–632 (1995)
7. J. Krim, I. Heyvaert, C. Van Haesendonck, Y. Bruynseraede, Phys. Rev. Lett. **70**, 57–61 (1993)
8. D. Berman, J. Krim, Thin Solid Films **520**, 6201 (2012)
9. G. Carbone, B. Lorenz, B.N.J. Persson, A. Wohlers, Eur. Phys. J. **29**, 275 (2009)
10. B. Lorenz, PGI, FZ Jülich, Germany
11. A. Wohlers, IFAS, RWTH Aachen, Germany
12. O. Albohr, Pirelli Deutschland AG, 64733 Höchst/Odenwald, Germany

13. A. Kovalev, S.N. Gorb, Department of Functional Morphology and Biomechanics, Zoological Institute at the University of Kiel, Germany
14. B.N.J. Persson, A. Kovalev and S.N. Gorb, Tribology Letters 10.1007/s11249-012-0053-2.
15. C. Ganser, F. Schmied, C. Teichert, Institute of Physics, Montanuniversität Leoben, Leoben, Austria
16. A. Kovalev, S.N. Gorb, Department of Functional Morphology and Biomechanics, Zoological Institute at the University of Kiel, Germany
17. B.N.J. Persson, A. Kovalev, M. Wasem, E. Gnecco, S.N. Gorb, EPL **92**, 46001 (2010)
18. D. Pires, B. Gotsmann, F. Porro, D. Wiesmann, U. Duerig, A. Knoll, Langmuir **25**, 5141 (2009)
19. D.E. Wolf, J. Villain, Europhys. Lett. **13**, 389 (1990)
20. F. Family, J. Phys. A **19**, L441 (1986)
21. C. Campana, B.N.J. Persson, M.H. Muser, J. Phys. Condens. Matter **23**, 085001 (2011)
22. S. Akarapu, T. Sharp, M.O. Robbins, Phys. Rev. Letters **106**, 204301 (2011)
23. B.N.J. Persson, M. Scaraggi, European J. Phys. E **34**, 113 (2011)
24. N. Mulakaluri, B.N.J. Persson, EPL **96**, 66003 (2011)
25. E. Bouchaud, J. Phys. Condens. Matter **9**, 4319 (1997)
26. E. Bouchaud, G. Lapasset, J. Planes, Europhys. Lett. **13**, 73 (1990)
27. T. Kessler, A. Visintin, A.E. Bolzan, G. Andreasen, R.C. Salvarezza, W.E. Triaca, A.J. Arivia, Langmuir **12**, 6587 (1996)
28. J. Krim, private communication